PCCP

ROYAL SOCIETY OF CHEMISTRY

PAPER

View Article Online
View Journal | View Issue



Cite this: *Phys. Chem. Chem. Phys.*, 2022, **24**, 23532

# Insights into cation–anion hydrogen bonding in mesogenic ionic liquids: an NMR study†

Debashis Majhi,[ab] Jing Dai[a] and Sergey V. Dvinskikh *[a]

The hydrogen-bonding interaction is studied in imidazolium-based mesogenic ionic liquids in their isotropic, smectic, and solid phases and in a nanoconfined state by proton solid-state nuclear magnetic resonance (NMR). In the smectic phase, the more basic anions form stronger hydrogen bonds. A small decrease of H-bonding in the mesophase with respect to that in the isotropic phase is associated with the presence of a layered assembly with high orientational order and limited conformational freedom. Hydrogen bond strength is not sensitive to the cation structural modification as long as the aprotic nature of the material is preserved. The strong cation–anion hydrogen bonding observed in the smectic phases provides direct support for the presence of ionic sublayers which form in ionic liquid crystals regardless of the location and alignment of the charged group in the cation, particularly irrespective of whether the charged group occupies a terminal or central position in the cation structure. A comparison of the results obtained in isotropic, liquid-crystalline, and solid states shows that in the bulk materials the dynamic state of ions ranging from high reorientational and translational freedom to partial orientation and positional order to full immobilization, respectively, has no strong impact on the cation–anion hydrogen bond strength. On the other hand, nanoconfinement of ionic liquid crystals led to hydrogen bond disruption due to competing interactions of anions with a solid interface.

Received 12th July 2022,
Accepted 5th September 2022

DOI: 10.1039/d2cp03188d

rsc.li/pccp



## Introduction

Ionic liquid crystals (ILCs) have the typical characteristics of ionic liquids (ILs) and, at the same time, a nano-scale-organized structure of liquid crystals.[1] This leads to the unique combination of the ionic conductivity of ionic liquids and the anisotropic physical and chemical properties of mesogenic (*i.e.* liquid-crystal forming) materials. The presence of orientational order in ILs results in remarkable dynamic properties exploited in modern technological applications.[2] Although intermolecular forces in these ionic materials are dominated by long-range non-directional electrostatic interactions, weaker and more local hydrogen-bonding (HB) interactions have a profound effect on mesophase stabilization and are fundamental for the properties of the mesogenic ionic liquids.[1–3] Also in conventional (non-mesogenic) ILs, the effects caused by hydrogen bonding have a significant influence on their physical properties and are crucial for practical applications.[4–7] Ionic H-bonds represent a wide area of research that is yet to be fully explored. Within a given IL, a variety of distinct HBs is formed between different types of sites in cations and anions which are the dominant HB donors and acceptors, respectively.[6] HB interactions have also been widely studied in nanoconfined ILs, presenting a class of hybrid composites combining the functional properties of ILs and porous solids.[8,9] Due to HB and other non-covalent interactions with the solid interface, confined ILs exhibit distinct structural, orientational, and dynamic preferences different from the bulk.

Mesophase occurrence in ILs is strongly related to a balance between hydrogen bonding, electrostatic interactions, and dispersion forces.[1] Because of a delicate equilibrium between these interactions, a small shift of the force balance can lead to discernible changes in the phase behaviour and ion local order and dynamics. Correlations have been revealed between the orientational order, mesophase window, and physicochemical properties of the anions such as ionic radius, charge delocalization, and the ability for hydrogen bonding.[1,10] Experimental data have been supported by extensive simulation studies of ILCs with a significant part devoted to understanding the impact of counterions on ordering properties.[11–13] Modification of the H-bonding network by hydration further contributes to mesophase stabilization despite decreasing the orientational order and accelerated ion translational dynamics.[14,15] The microscopic mechanism leading to the stabilization of the hydrated ionic smectic phase has been recently scrutinized by computational analysis.[16]

The most extensively studied ILCs are based on imidazolium cations.[17] Reduced ionic interactions due to charge delocalization

[a] *KTH Royal Institute of Technology, Stockholm, Sweden. E-mail: sergeid@kth.se*
[b] *Stockholm University, Stockholm, Sweden*

† Electronic supplementary information (ESI) available. See DOI: https://doi.org/10.1039/d2cp03188d

 

in the aromatic imidazolium core promote low transition temperatures, thereby increasing the application potential of the materials. Elucidating the hydrogen bonding contribution to intermolecular interactions in conventional non-mesogenic imidazolium-based ionic liquids has been a topic of a large body of experimental and computational research. X-Ray crystallographic studies in the solid state have shown that the acidic hydrogens in the imidazolium ring serve as H-bonding donors to form hydrogen bonds with anions.[4,18–20] The H-bonds mainly form at the H2 position and to a lesser extent at the H4,5 positions of the imidazolium ring, but also at weakly acidic hydrogens in the alkyl sidechains. In the isotropic liquid phase, the chemical shift (CS) in the nuclear magnetic resonance (NMR) spectra provides a sensitive probe of hydrogen bonding. Lungwitz *et al.* have shown that an anion-dependent differential $^{1}$H NMR shift is a direct measure of the strength of hydrogen bonding in imidazolium-based ILs.[21,22] Avent *et al.* reported one of the first evidence of HB in the liquid state and solution of ILs by multinuclear $^{1}$H, $^{13}$C, $^{35}$Cl, and $^{127}$I NMR.[23] The authors confirmed the formation of strong hydrogen bonds between halide anions and all three imidazolium ring protons and proposed a dynamic three-dimensional network of HB between anions and cations. Using proton NMR to study a large selection of imidazolium-based ILs, Cremer *et al.* concluded that hydrogen bonding was more pronounced for small and more strongly coordinating anions and was greatly reduced in the case of large and weakly coordinating anions.[24] Balevicius *et al.* investigated HB in the ionic liquid $C_{10}$mimBr in solution depending on solvent polarity and temperature.[25] Holbrey *et al.* studied proton chemical shifts related to HB in a series of $C_n$mim cations with varying alkyl chain lengths.[26] Thus, most experimental evidence of HB in IL-materials rested either on X-ray structural data in the crystalline state or NMR chemical shifts in the isotropic phase.

In addition to experimental observations, the impressive results on HB interactions in ILs and ILCs have been obtained by molecular dynamics (MD) simulations.[8,11–13,16,27–30] The MD analysis of the non-mesogenic ionic liquid $C_4$mimCl indicated that Cl is strongly localized in front of the acidic hydrogens in the imidazolium group.[30] Recent modelling of this material and its mixture with water has predicted a strong hydrogen bonding interaction between the C2–H2 moiety of imidazolium and the chloride anions.[29] Chlorides were also found to coordinate imidazolium in the vicinity of the C4–H4 and C5–H5 bonds. In the modelling of hydrated ILs, it has been shown that water molecules acted as hydrogen-bonded links between chloride anions.[29] Recently, a monohydrated ionic smectic phase of $C_{14}$mimCl·$H_2O$ has been studied.[16] It has been shown that water partly replaces the chloride anions in hydrogen bonding with the acidic protons of the imidazolium ring. MD analysis was also used to understand the interaction between the confined ILs and the pore wall surface and, thus, to study the effects of the pore size and geometry, the surface roughness, and the pore loading on the local structure and dynamics.[8]

Hydrogen bonds in the imidazolium-based ILs with various anions such as $Cl^-$, $Br^-$, $BF_4^-$ have been studied by density-functional theory (DFT) methods.[25,29,31–33] The structures of not only single ion pairs but also multiple ion pairs have been investigated.[32] In the case of halide counterions, DFT studies showed the formation of the HB network. A comparison of experimental and DFT data has shown that HB formation was associated with decreasing CS of imidazolium protons.[31] In many cases, very good agreement between the calculated and experimental spectra of neat ILs has been achieved in both qualitative and quantitative terms.[29–31] Effect of HB between anions and water on proton shielding in imidazolium cations was found to be in almost quantitative agreement with the experimental data.[30] The changes in CS observed in $^{1}$H and $^{13}$C NMR spectra of $C_{10}$mimBr with increasing solvents polarity and temperature have been explained by applying the model of the lengthening of the H2$\cdots$Br$^-$ hydrogen bond.[25]

Previously we have investigated the effects of HB forces on the dynamic and the orientational ordering behaviour of ILCs using dipolar NMR spectroscopy and diffusion NMR.[10,14,15] We have shown that the HB interaction between cations and anions has a profound effect on the mesophase stability and the molecular orientational order.[10] Modification of the HB network by hydration stabilizes the smectic phase in a wider temperature range compared to anhydrous materials.[14] A denser H-bond network in the presence of water molecules also led to increased anisotropy of the cation translation dynamics.[15] It has been also demonstrated that, despite strong homonuclear proton dipolar couplings, well-resolved proton spectra in highly ordered ionic smectic phases can be obtained using magic angle spinning (MAS) NMR, which opens up possibilities to exploit proton CS to probe the hydrogen bonding in ILCs with high sensitivity.[34,35]

The goal of the present study is to examine cation–anion hydrogen-bonding interactions in imidazolium-based mesogenic ILs. The molecular structures of the investigated IL materials are provided in Scheme S1 in the ESI.† Our primary experimental approach is solid-state $^{1}$H NMR spectroscopy to access proton chemical shift interactions in H-bonding centres. We perform measurements and compare HB effects in isotropic, liquid crystalline, and solid phases of ILCs as well as in the nanoconfined state. The influence of anion properties, cation structures, and ion dynamics and orientational order on HB strength is discussed.

## Materials and methods

The samples of ionic mesogenic materials with the cation $C_{12}$mim (1-dodecyl-3-methylimidazolium) and different anions, $Cl^-$, $Br^-$, $I^-$, and $BF_4^-$, were purchased from ABCR GmbH, Germany. Symmetrically substituted ILCs bis-1,3-dodecyl imidazolium bromide ($C_{12}$im$C_{12}$Br) and tetrafluoroborate ($C_{12}$im$C_{12}BF_4$), dicationic 3,3′-(1,6-hexanediyl)bis(1-dodecylimidazolium)dibromide ($C_6(C_{12}im)_2Br_2$) and di-tetrafluoroborate ($C_6(C_{12}im)_2(BF_4)_2$), and protic ILCs 1-dodecyl-imidazolium tetrafluoroborate ($C_{12}$im$BF_4$) and chloride ($C_{12}$imCl) were synthesized as described in the ESI.† Cation structures and atom labelling are

shown in Scheme S1 in the ESI.† All samples form a smectic A phase. Orientational order and cation conformation in these materials have been characterized in our previous studies using dipolar NMR methods.[10,36,37] The phase transition temperatures and residual water contents in the investigated samples are compiled in Table S1 in the ESI.†

IL/porous solid composites were prepared either by the post-impregnation method or the template synthesis method. The latter method delivers a material with fully loaded pores and a negligible amount of ex-pore ions. In the former one, the pore loading, while can be flexibly adjusted, is less defined, and a significant part of ex-pore ions and bulk ILs can be present in the sample. Mesoporous silica MCM41 with hexagonally ordered cylindrical pores of an average size of 2.4 nm was purchased from SigmaAldrich. Nanoporous silica KIT6 with a 3D bicontinuous cubic structure and an average pore diameter of 8.2 nm was synthesized as described in the ESI.† Procedures for the synthesis of the IL-templated MCM-41 composite and preparation of the nanoconfined ILCs by the post-impregnation method are presented in the ESI.†

Proton NMR measurements were carried out on a Bruker Avance-HD 500 spectrometer at the proton resonance frequency of 500 MHz using a TXI probe for isotropic liquid samples and a 4 mm MAS probe for materials in liquid-crystalline and solid states. $^{1}$H chemical shift was referenced to neat tetramethylsilane by use of the shift in adamantane $\delta_{iso}(^{1}H)$ = 1.85 ppm as a secondary chemical shift standard.[38] Two-dimensional $^{1}$H-$^{13}$C heteronuclear correlation (HETCOR)[39] spectra were recorded at the resonance frequencies of 500 and 125 MHz for $^{1}$H and $^{13}$C, respectively, and at the sample spinning speed of 8 kHz. Additional details are given in the ESI.†

## Results and discussion

### Hydrogen bonding in the isotropic phase of mesogenic ILs

In this section, we examine the relationship between $^{1}$H chemical shifts and cation–anion HB interactions in the isotropic phase of ILC samples. Such a correlation in non-mesogenic ILs has been reported for liquids based on a $C_8$mim cation and a wide range of anions.[24] These experiments were performed using neat materials and at room temperature to rule out solvent and temperature effects. However, longer chain mesogenic ILs at ambient temperature are typically in a solid or liquid-crystalline state. Furthermore, clearing points (transition temperatures from liquid crystals to isotropic liquids) of such mesogens vary in a wide range depending on the structure of cations and anions. Commonly in liquid crystals research, the properties of materials are compared at temperatures referenced to clearing points $T_c$. To follow this practice, we compared NMR spectra of ILCs recorded in the isotropic phase at temperatures ≈5 °C above their respective $T_c$. While $^{1}$H CS exhibited noticeable temperature dependence, this effect in most discussed cases is smaller compared to the changes induced by HB interactions. Besides, the effect of temperature difference on the results of the analysis can be partly compensated by relating the CS to that of the sites with no or negligible HB ability.

**Effect of the anion structure.** Chemical shifts of protons in the imidazolium group of the $C_{12}$mim cation increase in the anion sequence $BF_4$ < I < Br < Cl, essentially in the order of increasing the hydrogen bonding ability of the anions (Fig. 1). Such a trend has been previously confirmed in the NMR study of shorter chain imidazolium-based ILs.[24] The effect is evidently stronger for H2 protons compared to H4,5. This is supported by DFT computation that has shown a higher probability of structures with the anion positioned near the H2 atom compared to structures with the anion close to the H5 and/or H4 atoms.[33] Also, recent MD simulations confirmed the greater capacity of the C2–H2 moiety for hydrogen bonding as compared to that of C4–H4 or C5–H5.[29,30] A smaller but significant effect is also seen for aliphatic protons in the proximity of the imidazolium head. CSs of other protons in the chain are not affected by the anion substitution. In hydrated ILs, the cation–anion HB is outcompeted by the H-bonding of the anions with water molecules. Fig. S1 in the ESI† compares $^{1}$H spectra in the anhydrous and the monohydrated ILC $C_{12}$mimBr. Decreasing $^{1}$H CS in the monohydrated samples suggests weakening cation–anion H-bonding. Further decrease is expected at higher hydration levels and in diluted salts, similarly to the behaviour found in isotropic short-chain ILs.[29] The formation of hydrogen-bonded complexes between chloride anions and water molecules in hydrated ILs has been proven by MD simulations.[29]

In summarizing, our measurements in the isotropic phase of ILCs, despite the temperature limitation imposed by the phase behaviour, essentially reproduces the tendencies reported for conventional non-mesogenic ILs.

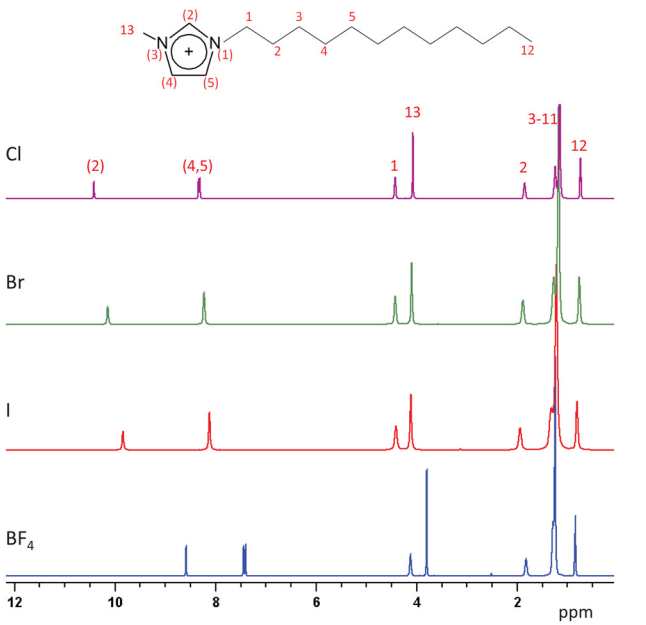


Fig. 1 Proton NMR spectra in the isotropic phase of ILCs $C_{12}$mimX (X = $BF_4$, I, Br, Cl) at the temperatures ≈5 °C above respective clearing temperatures.

**Effect of the cation structure.** The accessibility of potential H-bonding sites can be influenced by the position of the polar group within the cation and by the structure and size of substituting moieties. Holbrey *et al.* studied a series of $C_n$mim-based ILs and found that the proton CS related to HB was relatively insensitive to an alkyl chain length with $n$ = 0–18.[26] We have previously studied ordering properties of ILCs based on a symmetrically substituted imidazolium cation $C_{12}imC_{12}$ with two long alkyl chains.[36] The distinct structural feature of this material is the central position of the polar group contrasted to its terminal location in methyl-imidazolium analogues. Similarly, in ILCs based on the $C_6(C_{12}im)_2$ dication, there are two centrally located imidazolium groups connected by a flexible linker (see the cation structure in the ESI†). Proton NMR spectra in the isotropic phase of ILCs based on $C_{12}$mim and $C_{12}imC_{12}$ cations and $C_6(C_{12}im)_2$ dication are compared in Fig. 2. CSs of protons in the imidazolium ring are only slightly dependent on the structure of substitution units and the location of the polar group. This observation suggests that the HB strength is not influenced by the location of the charged moiety in the cationic structure irrespective of whether the charged group takes a terminal or central position. The effect is small for both weakly and strongly coordinating anions. Likewise, the presence of two charged groups in the dication has a negligible effect on the HB ability. Somewhat counterintuitively, possible steric effects do not alter the potential for H-bonding, and the charged groups are well exposed to the cation–anion association in these materials. Such behaviour in the isotropic liquid phase can be attributed to the high conformation freedom of these flexible cations. For example, the predicted U-shape conformation of cations makes charged group well accessible for anion H-bonding.[40,41] On the other hand, in the smectic phase discussed below, the layered assembly of cations may impose constraints on cation conformational dynamics and alignment of the imidazolium group and the side chains.[10,36,37]

In protic ILCs based on the cation $C_{12}$im, the primary centre for HB is shifted to NH protons and thus HB to CH protons weakens.[6] A significant decrease of CS of CH protons in the ring is observed for the salt with Cl anion compared to that in its aprotic counterpart (Fig. 3). Expectedly, no change of CS for CH protons in this cation is found in the case of $BF_4$ counterion exhibiting a weak HB capability (Fig. S2 in ESI†).

## Hydrogen bonding in the mesophase

In the smectic phase, proton spectra of static samples are strongly broadened by homonuclear dipolar interactions (Fig. S3, ESI†). To achieve $^1$H chemical resolution, magic angle sample spinning (MAS) was applied. The homonuclear dipolar interaction in axially rotating molecules in liquid crystals exhibits properties of an inhomogeneously broadened system[42] and is efficiently averaged by MAS even at a moderate spinning speed of the order of a few kHz.[34,35] Hence, the $^1$H MAS spectra in the mesophase display a high spectral resolution comparable to that in isotropic liquids, Fig. S3 (ESI†).

A small decrease of proton CS for the HB sites was observed at the transition from the isotropic to the smectic phase, Fig. 4. This suggests a decreasing potential for HB when the layered structure is formed in the smectic A phase. The effect is larger in the case of the strongly coordinating halide anions $Br^-$ and $Cl^-$ in comparison to that in the sample with anion $BF_4^-$. Conformational effects are not likely to be responsible for this difference; we have previously shown that the alignment of the alkyl chain and polar group in the $C_{12}$mim cation in the smectic phase is not sensitive to the anion type.[10,14] However, the observed changes of CS at the phase transitions are smaller than that related to other factors discussed above, such as cation and anion structures and hydration levels. It should be noted that a large difference in the chemical shift between the isotropic and the smectic phases of the static samples (typically reported for $^{13}$C or $^{15}$N spins)[43,44] is due to the contribution of the anisotropic part of the CS. Such a contribution is suppressed under MAS conditions. In the case of halide anions ($Br^-$, $Cl^-$), mesophasic windows are significantly larger (Fig. 4) because of the profound effect of these strongly coordinating

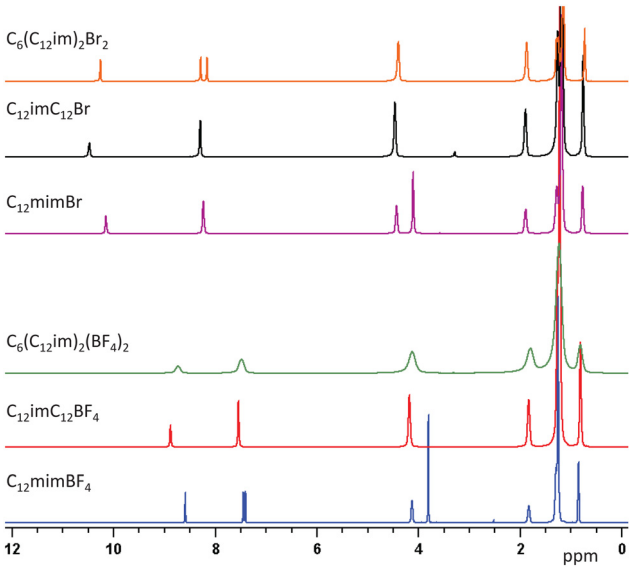


Fig. 2 Effect of cation structure on proton chemical shift of cations. Proton NMR spectra of cations $C_{12}$mim, $C_{12}imC_{12}$, and $C_6(C_{12}im)_2$ are compared in the isotropic phase.

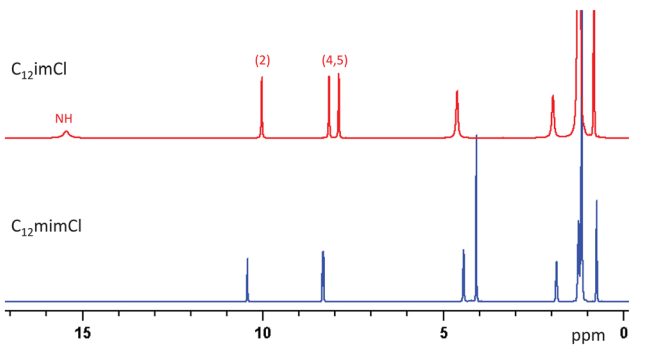


Fig. 3 Effect of protic substitution. Proton NMR spectra are compared in $C_{12}$mimCl (bottom) and $C_{12}$imCl (top) in the isotropic phase.

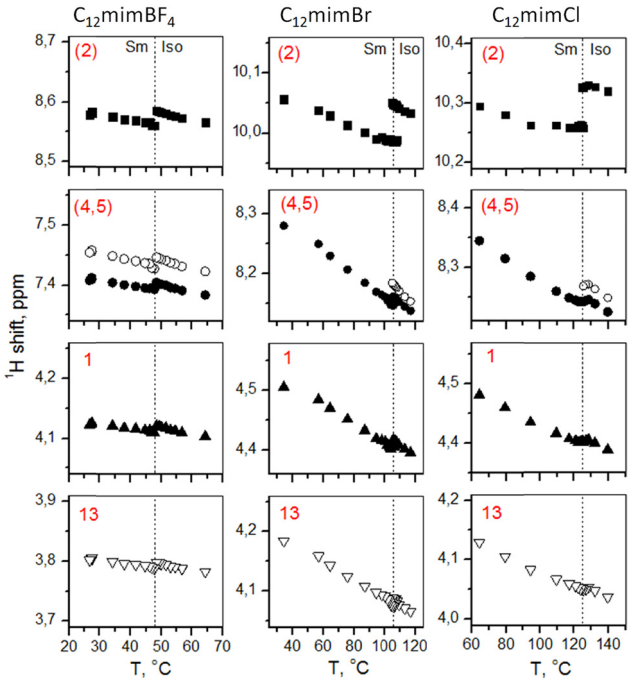


Fig. 4 Proton chemical shifts in the isotropic and smectic phases in $C_{12}$mimX (X = $BF_4$, Br, Cl) measured in the $^1$H MAS NMR experiment.

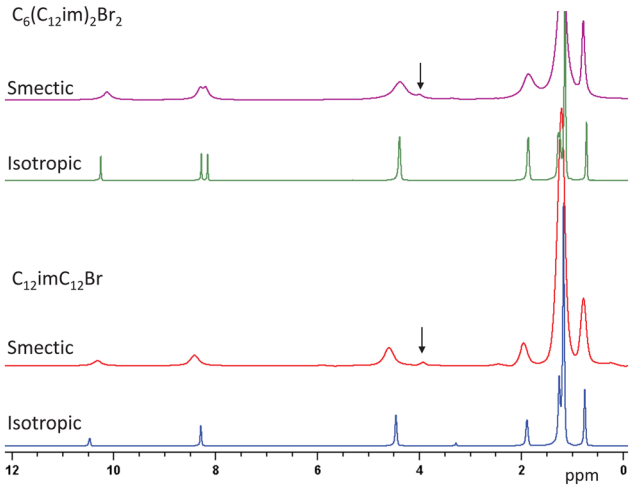


Fig. 5 Proton CS in isotropic and smectic phases in $C_{12}$im$C_{12}$Br and di-cationic $C_6(C_{12}im)_2Br_2$. Since for these samples, the clearing temperatures were above the safe operating limit of the MAS probe, we compared spectra in the smectic phase obtained using the MAS probe-head and spectra in the isotropic phase measured in the standard solution NMR probe-head. Note that MAS samples exhibit a small water trace (pointed by arrows) resulting from moisture absorption during loading samples in MAS rotors.

ions on mesophase stabilization. Recent MD simulation has confirmed higher stability range of the smectic phase in ILC $C_{12}$mimCl compared to that in $C_{12}$mim$BF_4$.[12]

The proton CS in the $C_{12}$im$C_{12}$ cation and the $C_6(C_{12}im)_2$ di-cation (Fig. 5), both having centrally located charged moieties, is very similar to that of the $C_{12}$mim cation (the spectrum shown in Fig. 1). Hence, analogously to the behaviour in the isotropic phase, also in the smectic phase, the charged group location and its alignment to the phase director have no large impact on the possibility of cation–anion association *via* HB. This result further supports the concept of ionic sublayers formed in smectic ILCs irrespective of whether a charged group takes a terminal or central position in the cation structure.

The significance of HB interactions for mesophase stabilization in ILCs has been widely discussed.[1] For example, it has been shown that the temperature range of the smectic phase is strongly correlated with the HB ability of counterions.[14,45] In this context, the important finding is that strong HB previously proved in isotropic ILs is also preserved in the mesophase despite the layered assembly and the high molecular order. This strong HB network in the presence of the layered cation assembly is preserved due to the formation of "ionic sublayers" where anions can approach polar groups to form H-bonds. The concept of ionic sublayer originally applied to cations with a terminal position of the charged groups can be also extended for other cation geometries exhibiting, in addition, a large difference in the degree of orientational order and alignment of the polar group to the phase director.

The smectic phase preserves high translational and rotation molecular mobility comparable to that in the isotropic phase. It is interesting to compare HB extent in the highly dynamic and fragile HB network in the smectic and isotropic phases to that for fully immobilized ions in the rigid solid phase. $^1$H-$^{13}$C HETCOR experiments recorded in the solid phase indicated that HB is formed to an extent similar to that in the isotropic and smectic phases, Fig. S4 in the ESI.† Hence, the dynamic state of ions has no strong effect on the cation–anion HB interaction.

## Ionic liquid crystals at solid interfaces

When ILs are confined in nanoporous silica, the cation–anion HB can be locally disrupted by the anion H-bonding to the solid interface where, for instance, surface hydroxyl groups may serve as hydrogen donor centres.[46,47] Lungwitz *et al.* have reported on the upfield shift of CH protons of H-imidazolium in protic liquid HmimCl confined in Aerosil-type silica.[48] In their sample, the NH proton was the main HB-centre; however, the corresponding signal was not observed in the $^1$H spectrum, presumably due to exchange with water present in the porous material. The gradual upfield shift of CH protons in the imidazolium ring with decreasing pore loading was attributed to a decrease in the cation–anion interaction due to increasing anion/surface hydrogen bond strength. To the best of our knowledge, no such effect has been observed yet for imidazolium-based or other analogous aprotic ILs.

We synthesized porous silica composites of various morphologies loaded with ILCs based on $C_{12}$mim cations and different anions $BF_4$, Br, and Cl. Template-synthesis method delivers a composite with fully loaded pores and a negligible amount of ex-pore ions. Among samples prepared by the post-impregnation method, those with a lower pore loading were chosen for analysis to ensure that most ions interact with the

 

silica surface and thus the effect of HB breaking is maximized. No thermotropic mesomorphism was observed in our nanoconfined materials. Previously, the phase transitions in nanoconfined ILCs were detected in cases where a significant bulk component was present in the sample and in large pores where the inner part of IL exhibited bulk-like properties.[49]

Proton MAS NMR spectra in porous composites are displayed in Fig. 6. Despite significant line broadening due to strong homonuclear dipolar couplings, it was possible to resolve the signals of the protons in the cation head group and compare their chemical shifts to those in bulk ILCs. A greater spectral resolution of proton signals was achieved using the 2D $^{1}H$-$^{13}C$ HETCOR experiment, which also assisted peak assignment by the correlation of $^{1}H$ and $^{13}C$ resonances (Fig. S5 in ESI†). 2D HETCOR data were essentially consistent with the 1D proton spectra.

In the nanoconfined $C_{12}$mim$BF_4$, no changes of $^{1}H$ CS were observed with respect to that in bulk materials (Fig. 6a). This result is consistent with the weak HB ability of $BF_4^-$. On the other hand, a significant decrease of $^{1}H$ CS was found in the case of ILs with Br and Cl anions (Fig. 6b and c). Thus, the cation–anion HB interaction decreases due to competing interactions between halide anions and the solid interface. The effect can be partly compensated by the possibility of forming HB between cations and surfaces.[46,50,51] In the impregnated sample $C_{12}$mimCl/KIT6 (Fig. 6c), where the bulk component was not washed away completely, two sets of peaks are distinguished with the narrow peaks at larger chemical shifts assigned to the bulk-like component.

Proton CS can be used as a sensitive indicator of the formation of the surface layer (contact layer) distinguished from the bulk-like component, which can be localized in the central part of large pores. Kohler *et al.* speculated that in large pores the contact layer insulates the rest of ILC from the support;[49] this may lead to the presence of two $^{1}H$ peaks associated with a more dynamic phase in the pore centre and relatively immobile ions in the surface layer. Note that here we study the cations with long alkyl chains, therefore our observation is difficult to compare with those in studies of compact short-chain (non-mesogenic) ILs, for which liquid-like ion dynamics was observed even in small pores.[52]

A large body of MD simulations has been carried out to gain a molecular-level picture of the interaction between confined ILs and pore surfaces.[8] Yan *et al.* observed ordered structures of IL EmimBr at silicate plates with multiple HB between Br and surface hydroxyl groups.[53] Sieffert *et al.* compared nanoconfined BmimCl and Bmim$BF_4$ and found that $Cl^-$ anions are strongly hydrogen-bonded to silanol protons of the silica surface, while in the case of $BF_4^-$, the interaction energy is much smaller.[54] These results are essentially in agreement with our experimental data. DFT studies also indicated a (weak) attraction of imidazolium-based cations by the surface.[50,51] While the H-bonding between cations and surface groups was not evident from our NMR data, experimental FTIR studies have indicated the related shifts of C–H vibrational bands in the polar head.[50,51,55]

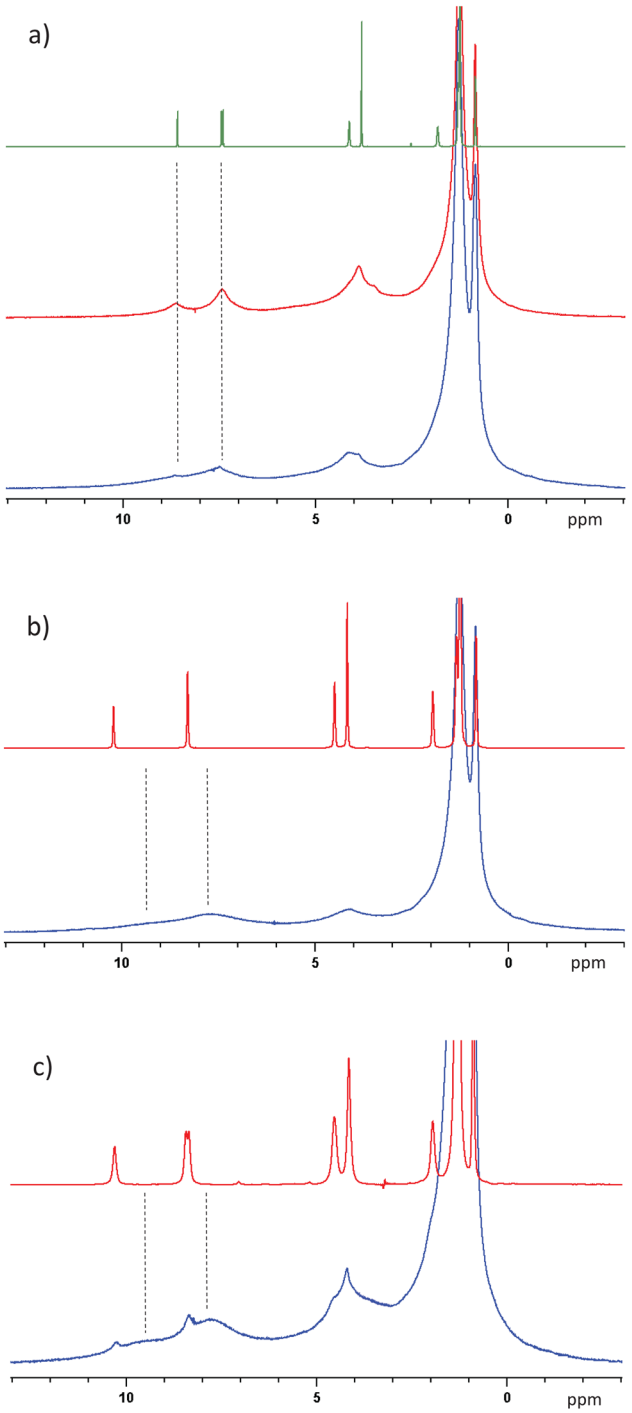


Fig. 6 (a) Ionic liquid $C_{12}$mim$BF_4$ templated in MCM41 (bottom), impregnated in KIT6 (middle), and the bulk sample in the isotropic phase (top). (b) $C_{12}$mimBr templated in MCM41 (bottom) and the bulk sample in the isotropic phase (top). (c) $C_{12}$mimCl impregnated in MCM41 (bottom) and the bulk sample in the smectic phase (top). Spectra in porous samples are measured at 12 kHz MAS.

## Conclusions

We have experimentally investigated hydrogen-bonding interactions in a series of imidazolium-based mesogenic ionic liquids in their isotropic, smectic, and solid phases and in a

nanoconfined state. Proton chemical shift is a sensitive diagnostic tool for the HB interaction in mesogenic ILs. Using MAS NMR, $^{1}$H CS in the liquid-crystalline state can be assessed with sensitivity and accuracy comparable to that in isotropic phases.

The presented results confirm, in line with the trend reported in the isotropic phase of non-mesogenic ILs,[24] that also in the smectic phase of ILCs, the smaller and more basic anions form stronger HB. The important new finding is that the extent of the HB interaction in the mesophase does not change significantly with respect to that in the isotropic phase. A relatively small but noticeable decrease of HB in the mesophase is associated with the presence of a layered assembly with high orientational order and limited conformation freedom. HB is not disrupted strongly in the mesophase due to the formation of ionic sublayers where anions can approach and interact with the cation polar groups and form H-bonds.

Remarkably, the HB strength is not sensitive to the cation structural modification as long as the aprotic nature of the material is preserved. The strong cation–anion HB observed in smectic phases provides direct support for the concept of ionic sublayers, which form in ILCs regardless of location and alignment of the charged group in the cation, particularly irrespective of whether the charged group occupies a terminal or central position in the cation structure. Hence, the concept of an ionic sublayer, while initially introduced for cations with terminal positions of polar groups, can be also extended to other cation geometries.

A comparison of the results obtained in the bulk material in isotropic, liquid-crystalline, and solid states has shown that the dynamic state of ions ranging from high reorientational and translational freedom to partial orientation and positional order to full immobilization, respectively, has no dramatic effect on cation–anion HB strength. On the other hand, nanoconfinement of ILCs led to local disruption of HB due to competing interactions of anions with solid interfaces.

## Author contributions

S. V. D. designed and proposed the methods. D. M. and S. V. D. performed the NMR measurements and analysis. J. D. and D. M. conducted the synthesis and characterization of materials. All authors contributed to the preparation of the manuscript.

## Conflicts of interest

There are no conflicts to declare.

## Acknowledgements

This work was supported by the Swedish Research Council VR (project no. 2017-04278).

## References

1 K. Goossens, K. Lava, C. W. Bielawski and K. Binnemans, *Chem. Rev.*, 2016, **116**, 4643–4807.
2 T. Kato, M. Yoshio, T. Ichikawa, B. Soberats, H. Ohno and M. Funahashi, *Nat. Rev. Mater.*, 2017, **2**, 17001.
3 A. A. Fernandez and P. H. J. Kouwer, *Int. J. Mol. Sci.*, 2016, **17**, 731.
4 K. Dong and S. J. Zhang, *Chem. – Eur. J.*, 2012, **18**, 2748–2761.
5 K. Fumino, T. Peppel, M. Geppert-Rybczynska, D. H. Zaitsau, J. K. Lehmann, S. P. Verevkin, M. Kockerling and R. Ludwig, *Phys. Chem. Chem. Phys.*, 2011, **13**, 14064–14075.
6 P. A. Hunt, C. R. Ashworth and R. P. Matthews, *Chem. Soc. Rev.*, 2015, **44**, 1257–1288.
7 K. Fumino, A. Wulf and R. Ludwig, *Angew. Chem., Int. Ed.*, 2008, **47**, 8731–8734.
8 S. G. Zhang, J. H. Zhang, Y. Zhang and Y. Q. Deng, *Chem. Rev.*, 2017, **117**, 6755–6833.
9 F. Borghi and A. Podesta, *Adv. Phys.: X*, 2020, **5**, 1736949.
10 J. Dai, D. Majhi, B. B. Kharkov and S. V. Dvinskikh, *Crystals*, 2019, **9**, 495.
11 N. Kapernaum, A. Lange, M. Ebert, M. A. Grunwald, C. Haege, S. Marino, A. Zens, A. Taubert, F. Giesselmann and S. Laschat, *ChemPlusChem*, 2022, **87**, e202100397.
12 G. Saielli, *Crystals*, 2020, **10**, 253.
13 H. Bartsch, M. Bier and S. Dietrich, *J. Chem. Phys.*, 2021, **154**, 014901.
14 D. Majhi, J. Dai, A. V. Komolkin and S. V. Dvinskikh, *Phys. Chem. Chem. Phys.*, 2020, **22**, 13408–13417.
15 S. V. Dvinskikh, *Liq. Cryst.*, 2020, **47**, 1975–1985.
16 G. Saielli, *Phys. Chem. Chem. Phys.*, 2021, **23**, 24386–24395.
17 L. Douce, J. M. Suisse, D. Guillon and A. Taubert, *Liq. Cryst.*, 2011, **38**, 1653–1661.
18 A. Khrizman, H. Y. Cheng, G. Bottini and G. Moyna, *Chem. Commun.*, 2015, **51**, 3193–3195.
19 S. Kohmoto, S. Okuyama, T. Nakai, M. Takahashi, K. Kishikawa, H. Masu and I. Azumaya, *J. Mol. Struct.*, 2011, **998**, 192–197.
20 K. Bouchmella, S. G. Dutremez, B. Alonso, F. Mauri and C. Gervais, *Cryst. Growth Des.*, 2008, **8**, 3941–3950.
21 R. Lungwitz, M. Friedrich, W. Linert and S. Spange, *New J. Chem.*, 2008, **32**, 1493–1499.
22 R. Lungwitz and S. Spange, *New J. Chem.*, 2008, **32**, 392–394.
23 A. G. Avent, P. A. Chaloner, M. P. Day, K. R. Seddon and T. Welton, *J. Chem. Soc., Dalton Trans.*, 1994, 3405–3413.
24 T. Cremer, C. Kolbeck, K. R. J. Lovelock, N. Paape, R. Wölfel, P. S. Schulz, P. Wasserscheid, H. Weber, J. Thar, B. Kirchner, F. Maier and H. P. Steinrück, *Chem. – Eur. J.*, 2010, **16**, 9018–9033.
25 V. Balevicius, Z. Gdaniec, L. Dziaugys, F. Kuliesius and A. Marsalka, *Acta Chim. Slov.*, 2011, **58**, 458–464.
26 J. D. Holbrey and K. R. Seddon, *J. Chem. Soc., Dalton Trans.*, 1999, 2133–2139.
27 B. Qiao, C. Krekeler, R. Berger, L. Delle Site and C. Holm, *J. Phys. Chem. B*, 2008, **112**, 1743–1751.
28 I. Skarmoutsos, T. Welton and P. A. Hunt, *Phys. Chem. Chem. Phys.*, 2014, **16**, 3675–3685.
29 D. Lengvinaite, S. Kvedaraviciute, S. Bielskute, V. Klimavicius, V. Balevicius, F. Mocci, A. Laaksonen and K. Aidas, *J. Phys. Chem. B*, 2021, **125**, 13255–13266.
30 G. Saielli, *Molecules*, 2020, **25**, 2085.

 

31 S. Chen, R. Vijayaraghavan, D. R. MacFarlane and E. I. Izgorodina, *J. Phys. Chem. B*, 2013, **117**, 3186–3197.
32 K. Dong, S. J. Zhang, D. X. Wang and X. Q. Yao, *J. Phys. Chem. A*, 2006, **110**, 9775–9782.
33 S. A. Katsyuba, T. P. Griaznova, A. Vidis and P. J. Dyson, *J. Phys. Chem. B*, 2009, **113**, 5046–5051.
34 D. Majhi, B. B. Kharkov and S. V. Dvinskikh, *Chem. Phys. Lett.*, 2021, **781**, 138997.
35 S. K. Mann, M. K. Devgan, W. T. Franks, S. Huband, C. L. Chan, J. Griffith, D. Pugh, N. J. Brooks, T. Welton, L. L. M. T. N. Pham, J. R. Lewandowski and S. P. Brown, *J. Phys. Chem. B*, 2020, **124**, 4975–4988.
36 D. Majhi, A. V. Komolkin and S. V. Dvinskikh, *Int. J. Mol. Sci.*, 2020, **21**, 5024.
37 D. Majhi and S. V. Dvinskikh, *Sci. Rep.*, 2021, **11**, 5985.
38 S. Hayashi and K. Hayamizu, *Bull. Chem. Soc. Jpn.*, 1991, **64**, 685–687.
39 B. J. vanRossum, H. Forster and H. J. M. deGroot, *J. Magn. Reson.*, 1997, **124**, 516–519.
40 X. J. Wang, C. S. Vogel, F. W. Heinemann, P. Wasserscheid and K. Meyer, *Cryst. Growth Des.*, 2011, **11**, 1974–1988.
41 L. Guglielmero, L. Guazzelli, A. Toncelli, C. Chiappe, A. Tredicucci and C. S. Pomelli, *RSC Adv.*, 2019, **9**, 30269–30276.
42 M. M. Maricq and J. S. Waugh, *J. Chem. Phys.*, 1979, **70**, 3300–3316.
43 M. Cifelli, V. Domenici, V. I. Chizhik and S. V. Dvinskikh, *Appl. Magn. Reson.*, 2018, **49**, 553–562.
44 J. Dai, B. B. Kharkov and S. V. Dvinskikh, *Crystals*, 2019, **9**, 18.
45 K. Damodaran, *Progr. Nucl. Magn. Reson. Spectrosc.*, 2022, **129**, 1–27.
46 G. J. D. Soler-Illia, C. Sanchez, B. Lebeau and J. Patarin, *Chem. Rev.*, 2002, **102**, 4093–4138.
47 M. N. Garaga, L. Aguilera, N. Yaghini, A. Matic, M. Persson and A. Martinelli, *Phys. Chem. Chem. Phys.*, 2017, **19**, 5727–5736.
48 R. Lungwitz and S. Spange, *J. Phys. Chem. C*, 2008, **112**, 19443–19448.
49 F. T. U. Kohler, B. Morain, A. Weiss, M. Laurin, J. Libuda, V. Wagner, B. U. Melcher, X. J. Wang, K. Meyer and P. Wasserscheid, *Chem. Phys. Chem.*, 2011, **12**, 3539–3546.
50 A. K. Gupta, Y. L. Verma, R. K. Singh and S. Chandra, *J. Phys. Chem. C*, 2014, **118**, 1530–1539.
51 M. P. Singh, R. K. Singh and S. Chandra, *Chem. Phys. Chem.*, 2010, **11**, 2036–2043.
52 R. Goebel, P. Hesemann, J. Weber, E. Moller, A. Friedrich, S. Beuermann and A. Taubert, *Phys. Chem. Chem. Phys.*, 2009, **11**, 3653–3662.
53 Z. F. Yan, D. W. Meng, X. L. Wu, X. L. Zhang, W. P. Liu and K. H. He, *J. Phys. Chem. C*, 2015, **119**, 19244–19252.
54 N. Sieffert and G. Wipff, *J. Phys. Chem. C*, 2008, **112**, 19590–19603.
55 M. P. Singh, R. K. Singh and S. Chandra, *J. Phys. Chem. B*, 2011, **115**, 7505–7514.